

The MIGDAL Experiment

Tim Marley

Imperial College London / Rutherford Appleton Laboratory

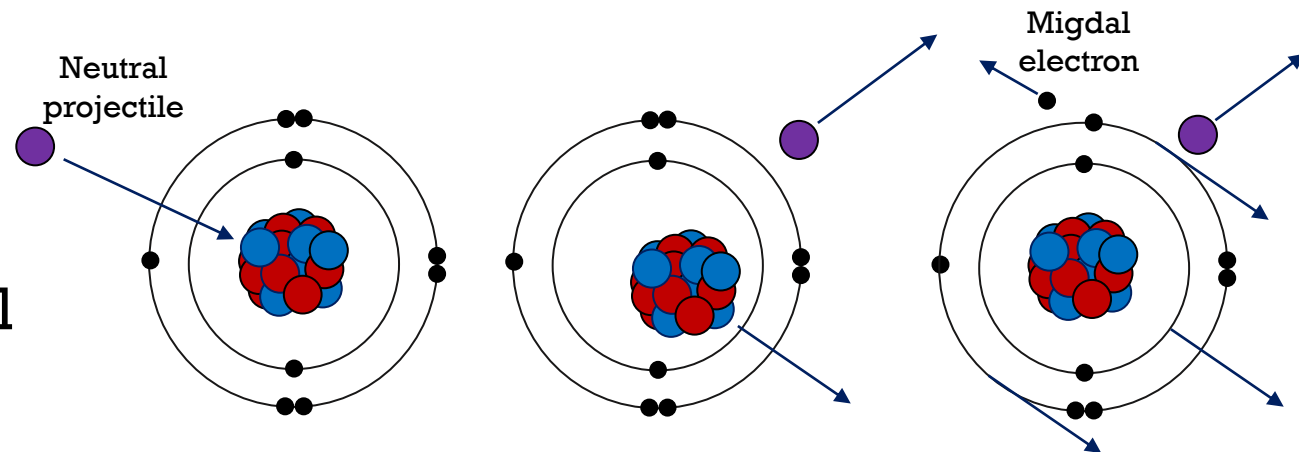
On behalf of the MIGDAL collaboration

7th International Conference on Micro Pattern Gaseous Detectors – 12-16 December 2022 – Rehovot, Israel

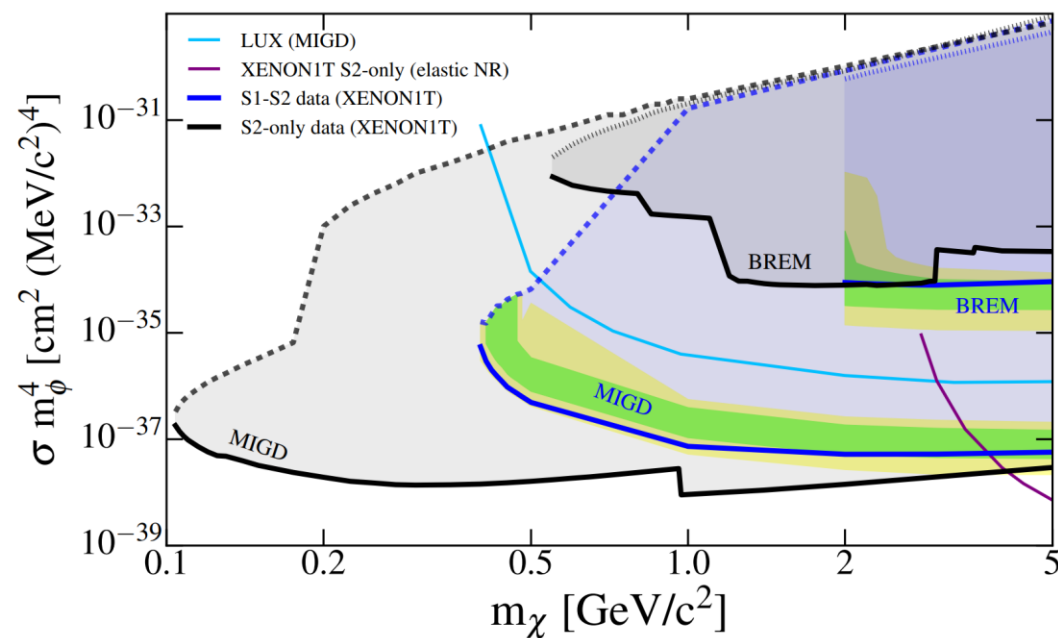


The Migdal effect

- Direct DM experiments exploit the Migdal effect to search for nuclear recoils below threshold.
- This rare atomic effect was predicted by A. Migdal in the 30's/40's and first observed in radioactive decays in the 70's – but not yet recorded in nuclear scattering.
- We aim to achieve the unambiguous observation (and characterisation) of the Migdal effect using a low-pressure optical TPC.

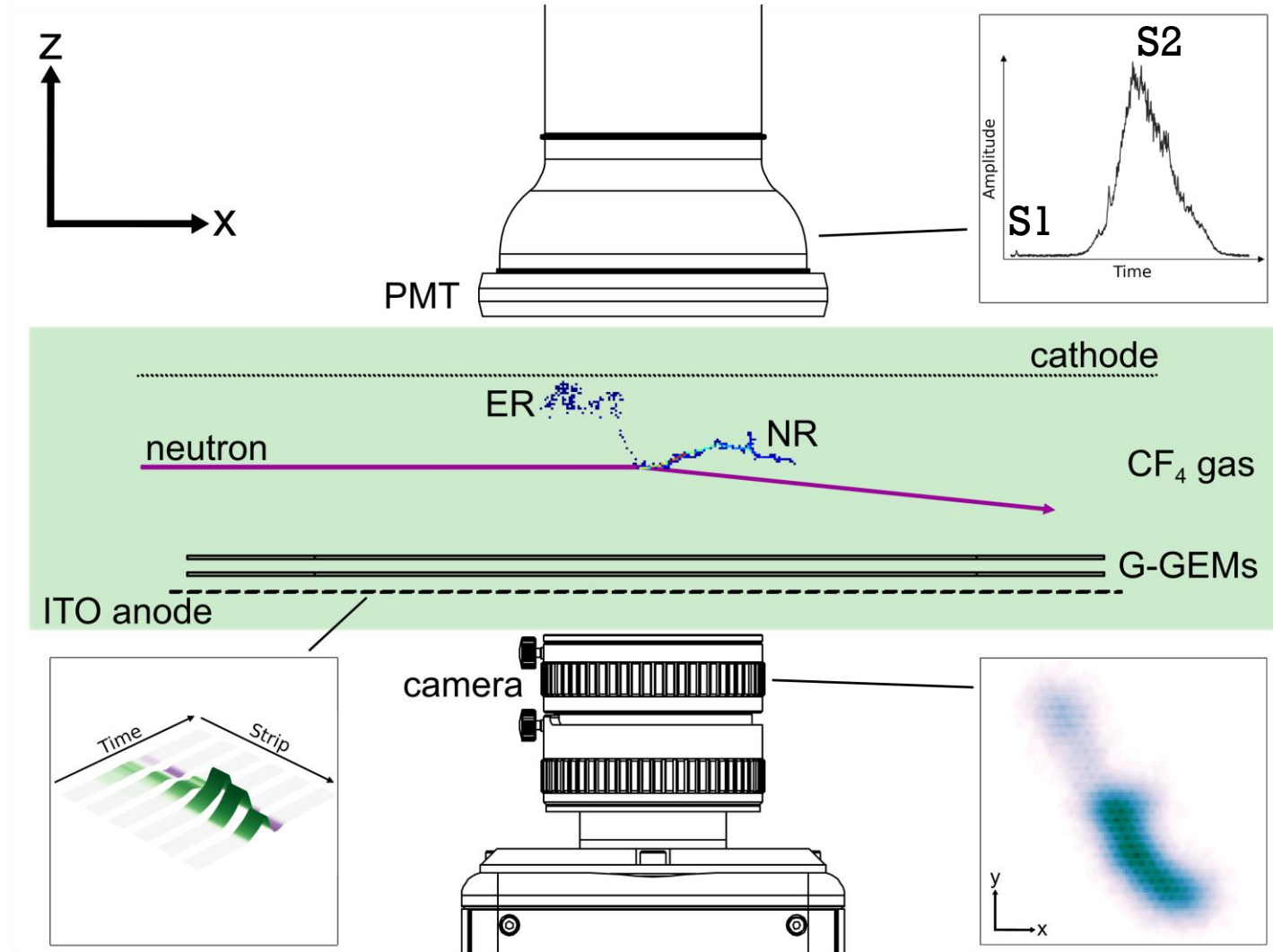


Migdal topology involves an electron and a nuclear recoil originating from the same vertex.

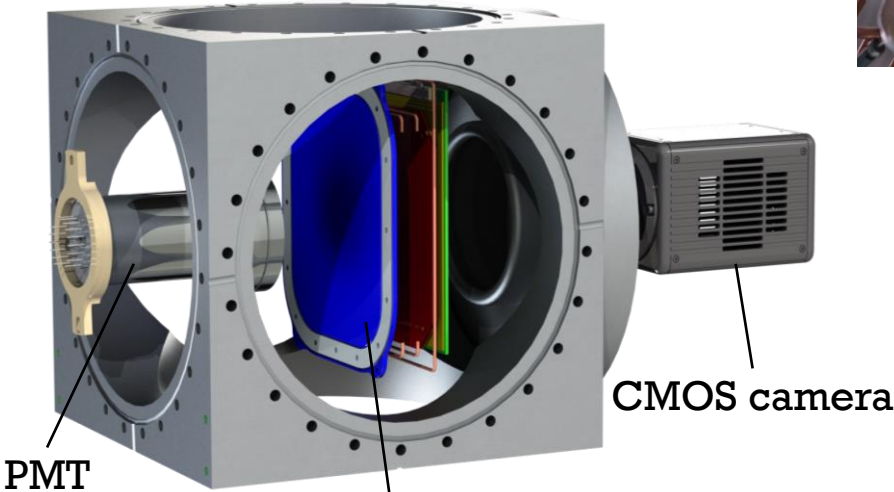
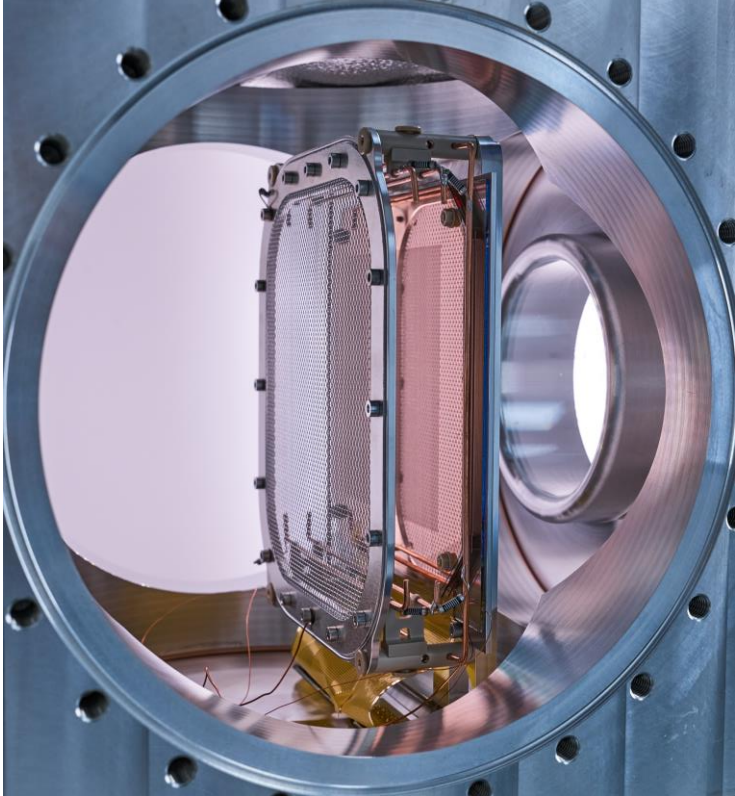


The MIGDAL experiment

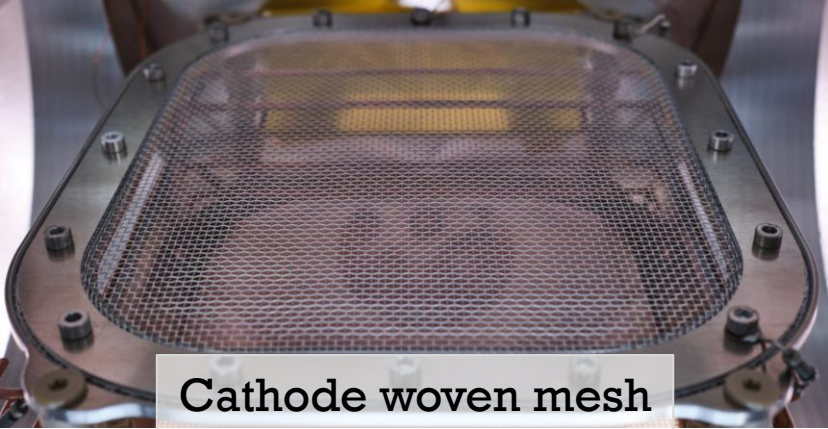
- Low-pressure gas: 50 Torr of CF_4
 - Extended particle tracks
 - Avoid photon interactions
 - Can work with fraction of Ar
- Optical TPC
 - Amplification: 2x glass-GEMs
 - Optical: camera + photomultiplier tube
 - Charge: 120 ITO anode strips
- High-yield neutron generator
 - D-D: 2.47 MeV (10^9 n/s)
 - Defined beam, “clear” through TPC
- Electron and nuclear recoil tracks
 - Migdal: NR+ER tracks, common vertex
 - NR and ER have very different dE/dx
 - 5 keV electron threshold (Fe-55 calibration)



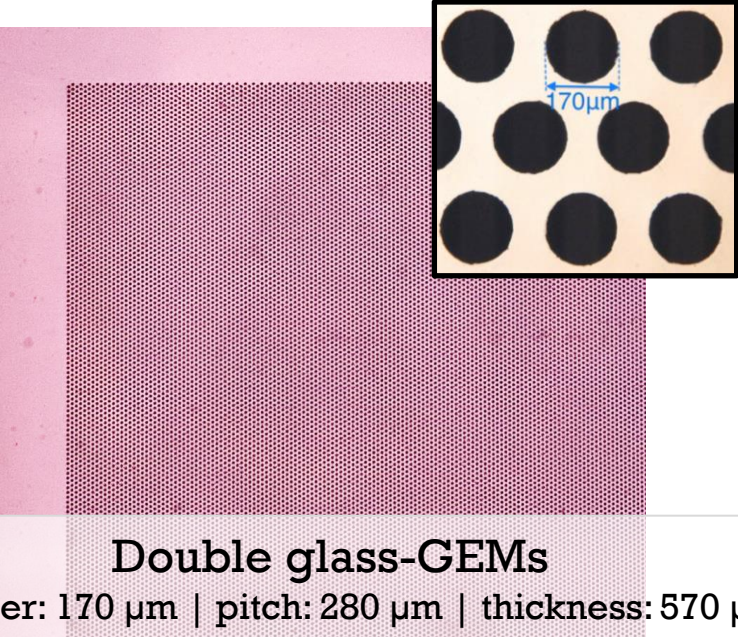
The MIGDAL optical-TPC



Cathode, GEM stack, ITO
10×10×3 cm³ active region
(compact!)



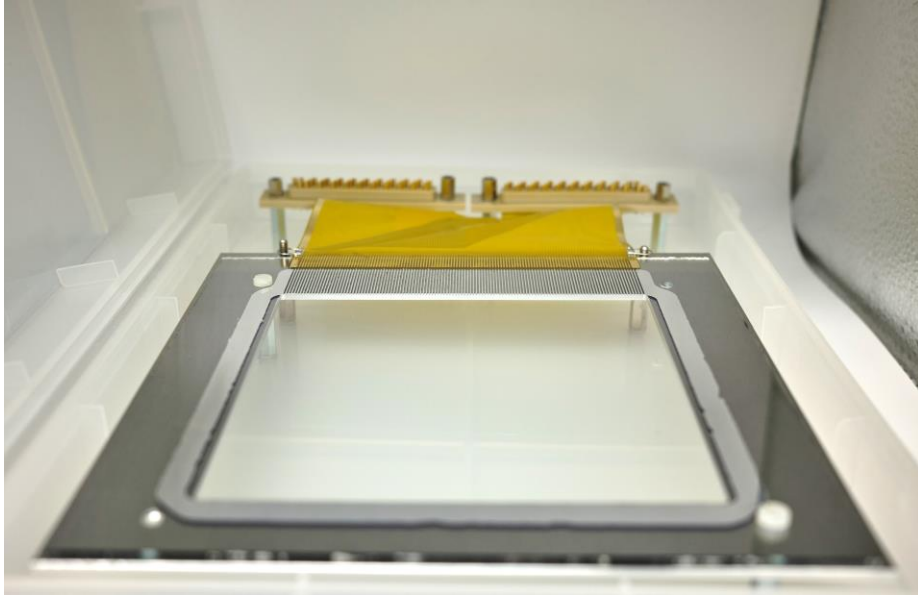
Cathode woven mesh
280 μm Al wire



Double glass-GEMs
Diameter: 170 μm | pitch: 280 μm | thickness: 570 μm

Detector readout

Charge readout



ITO anode strips

Post-GEM ionisation

Readout of (x,z) plane

Pitch: 833 μm

Digitised at 2 ns/sample

(Drift velocity: 130 $\mu\text{m}/\text{ns}$)

Optical readout



sCMOS camera

(**Hamamatsu ORCA-Fusion**)

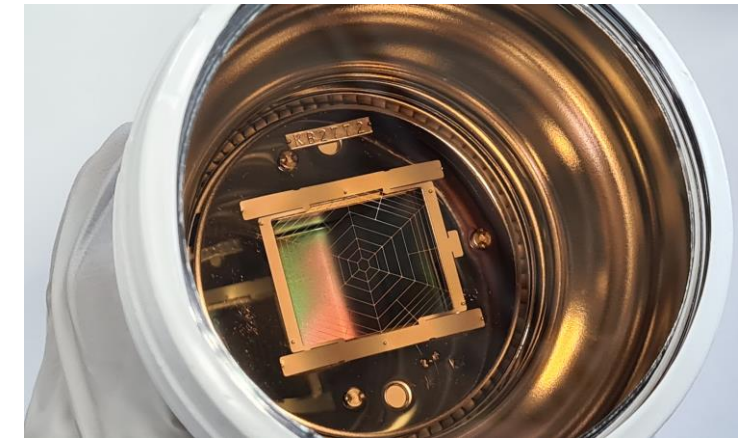
Detects GEM scintillation through glass viewport behind ITO anode

Readout of (x,y) plane

Exposure: 11.2 ms/frame (continuous)

Px scale: 43 μm

Lens: EHD-25085-C; 25mm f/0.85



VUV PMT (Hamamatsu R11410)

Detects primary and secondary (GEM) scintillation

Absolute depth (z) coordinate

Digitised at 2 ns/sample

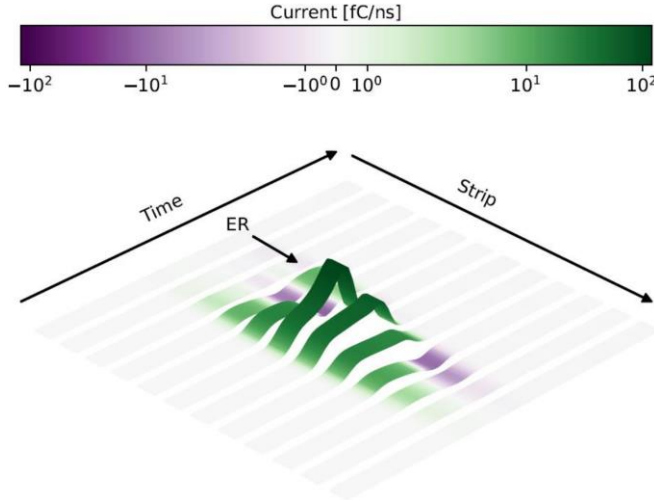
[Trigger]

End-to-end simulation

- DEGRAD (electron track)
- TRIM (NR cascade and electronic dE/dx)
- Magboltz (drift properties)
- Garfield++ (GEMs)
- Gmsh/Elmer & ANSYS (ITO and E-field)

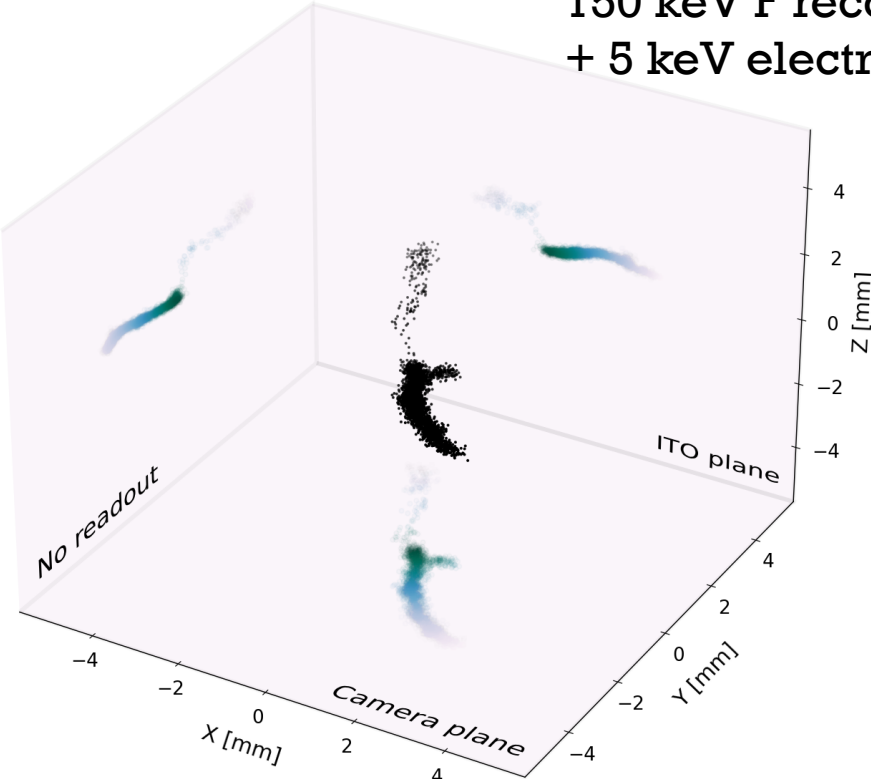
Anode strip readout

Induction/collection
(electronics deconvolved)



Migdal event

150 keV F recoil
+ 5 keV electron



Camera readout

Diffusion + GEMs + noise

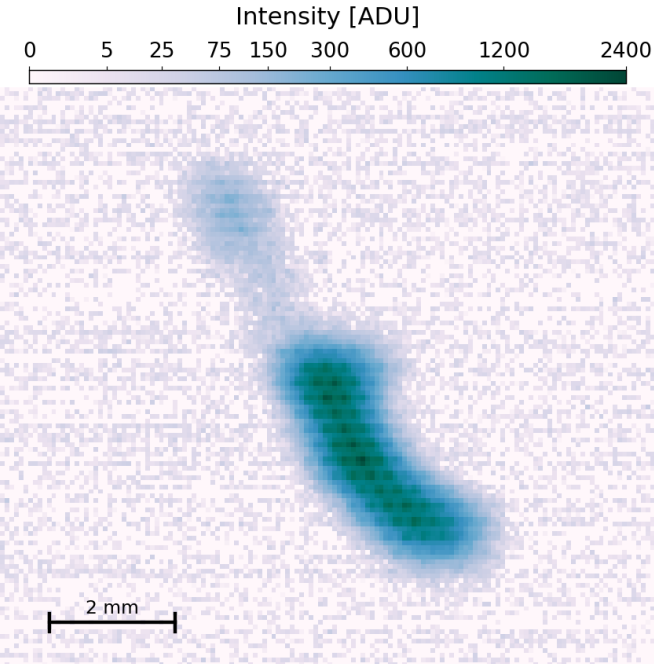
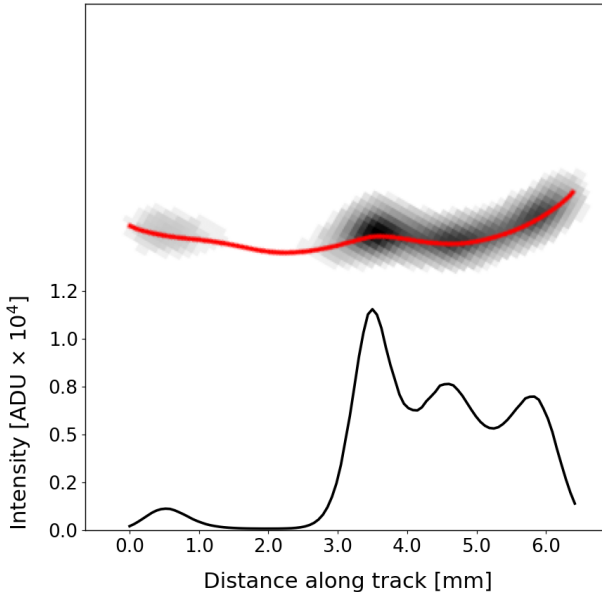


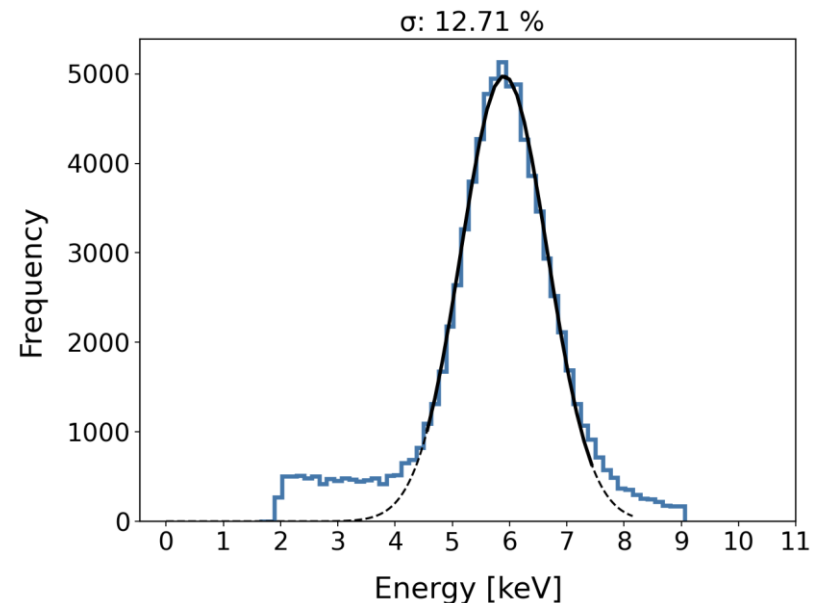
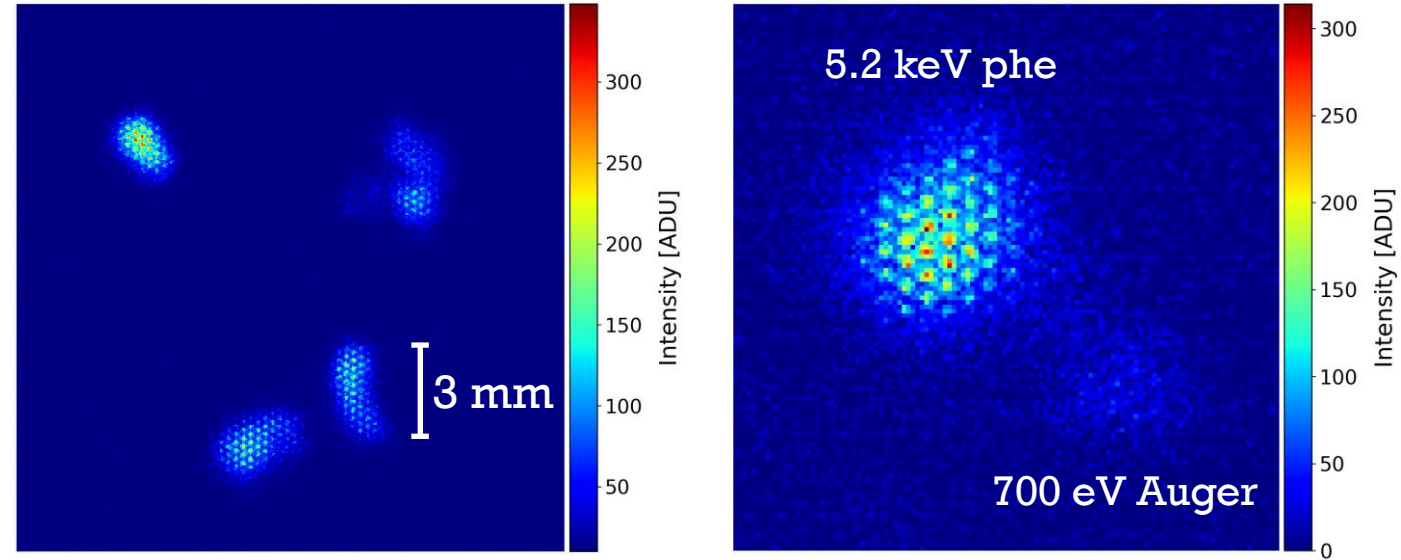
Image analysis

Deconvolution + RidgeFinder



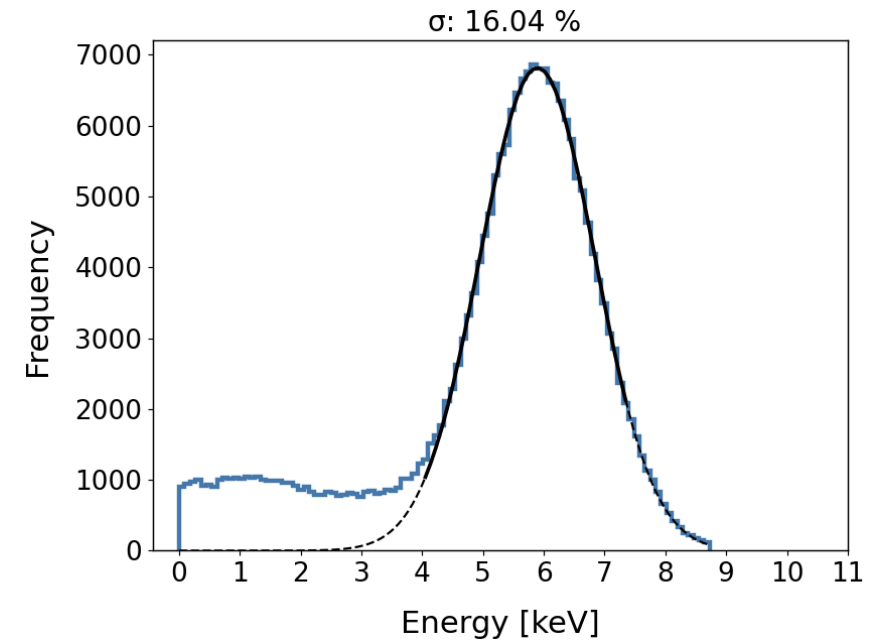
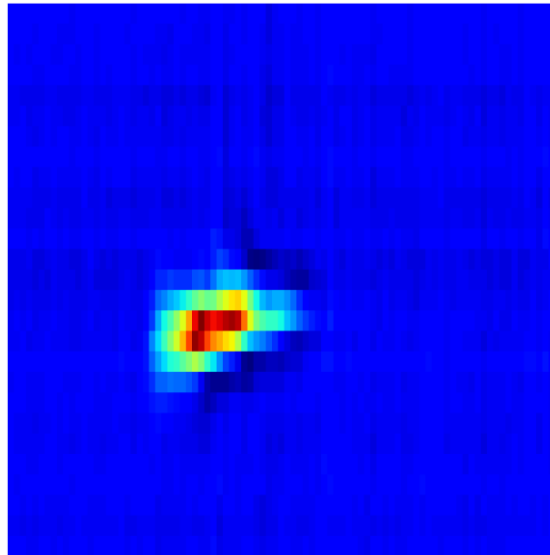
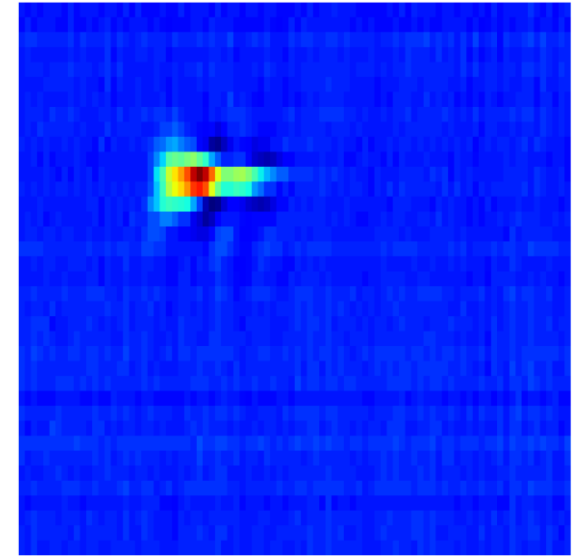
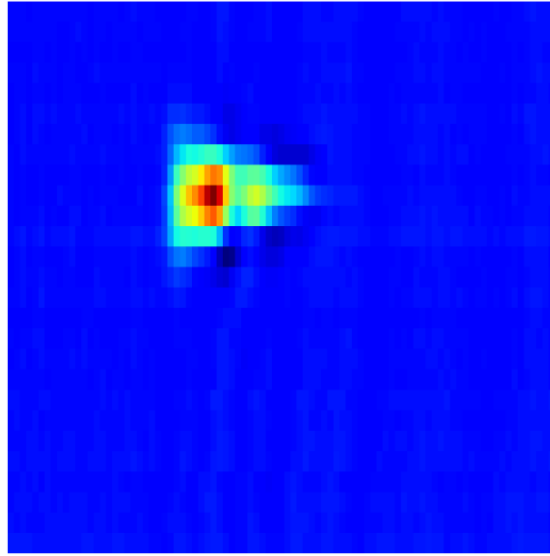
Calibration with ^{55}Fe – Pure CF_4

- Tests were performed with ^{55}Fe (5.9 keV x-ray).
- The gain was pushed high.
- Head & tail is clearly resolved.
- 700 eV Auger electron from fluorine is visible.
- Achievable energy resolution is high ($\sigma/\mu \sim 12.7\%$).
- *See Elizabeth's talk on Thursday for 3D reconstruction!*



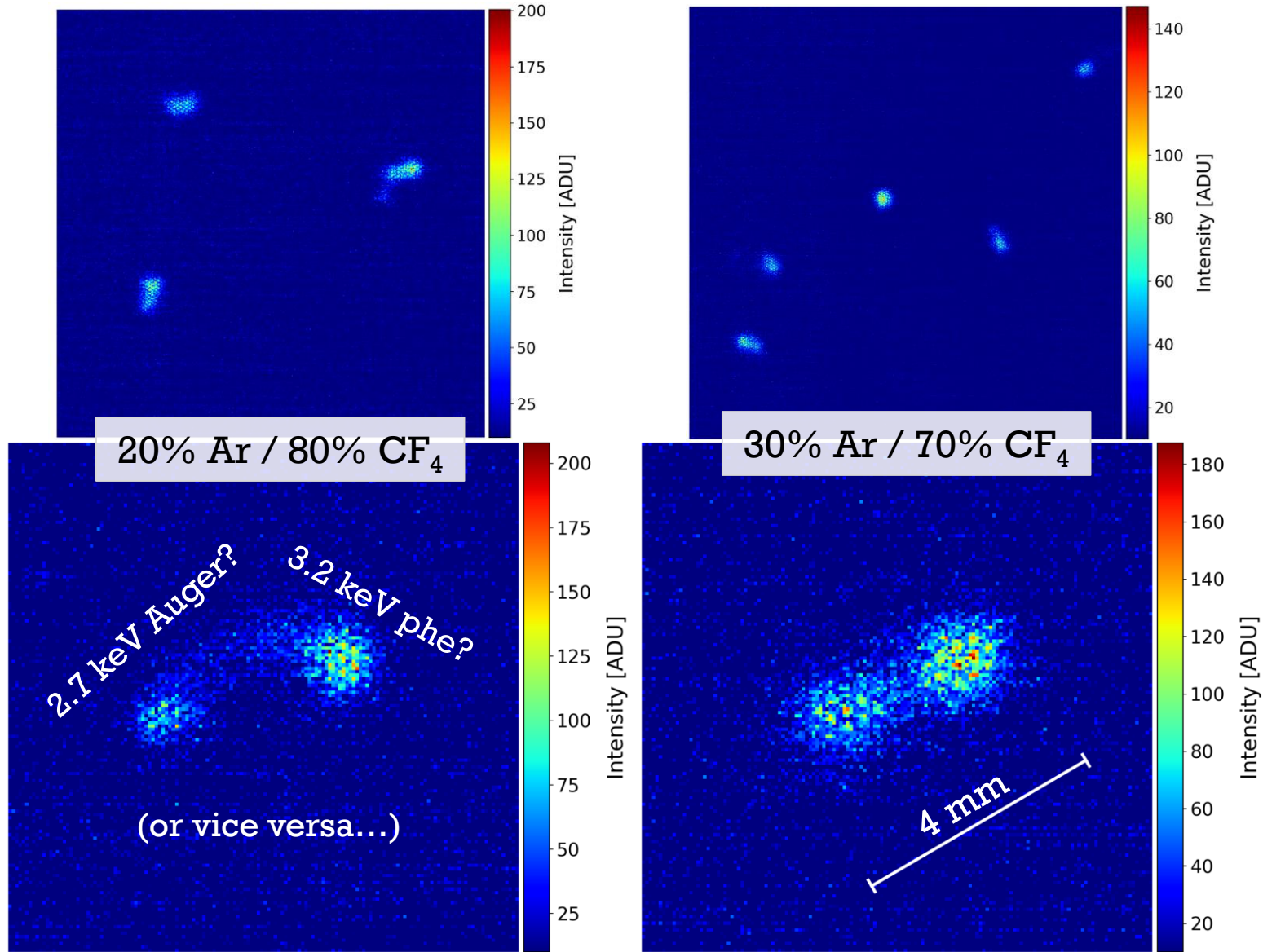
ITO (Pure CF_4)

- Very good signal to noise.
- Spatial resolution is not as good as camera (~ 0.83 mm pitch).
- Good energy resolution even with no flat fielding correction.
- Analysis of ITO images is ongoing, methods are still being refined.



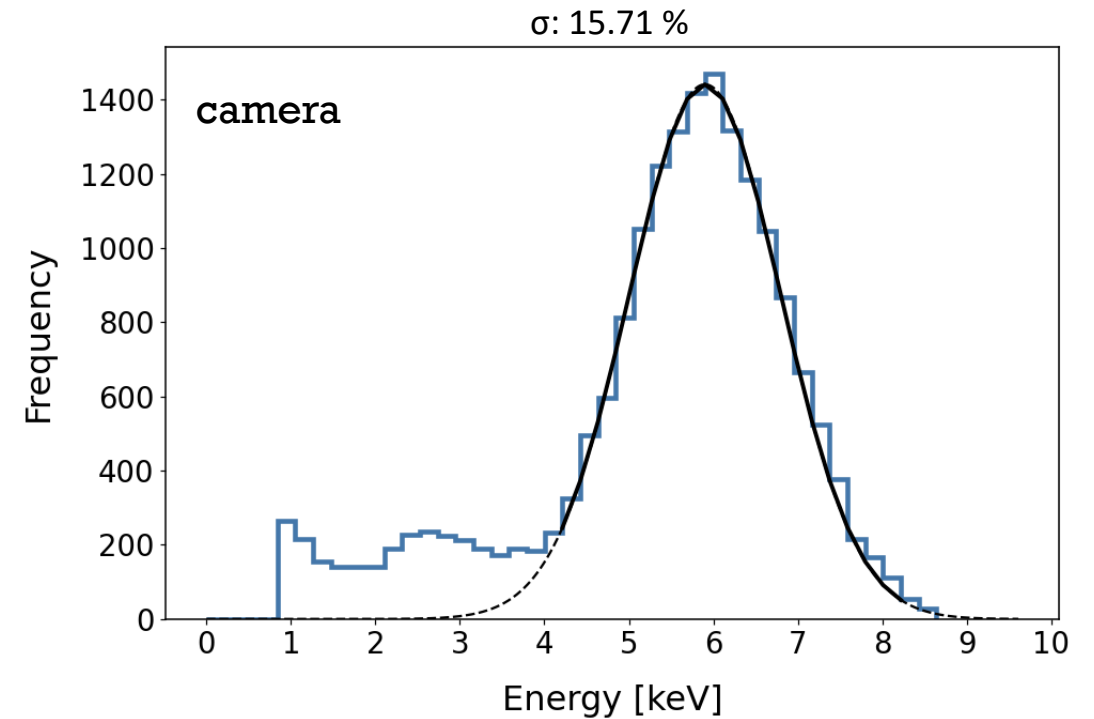
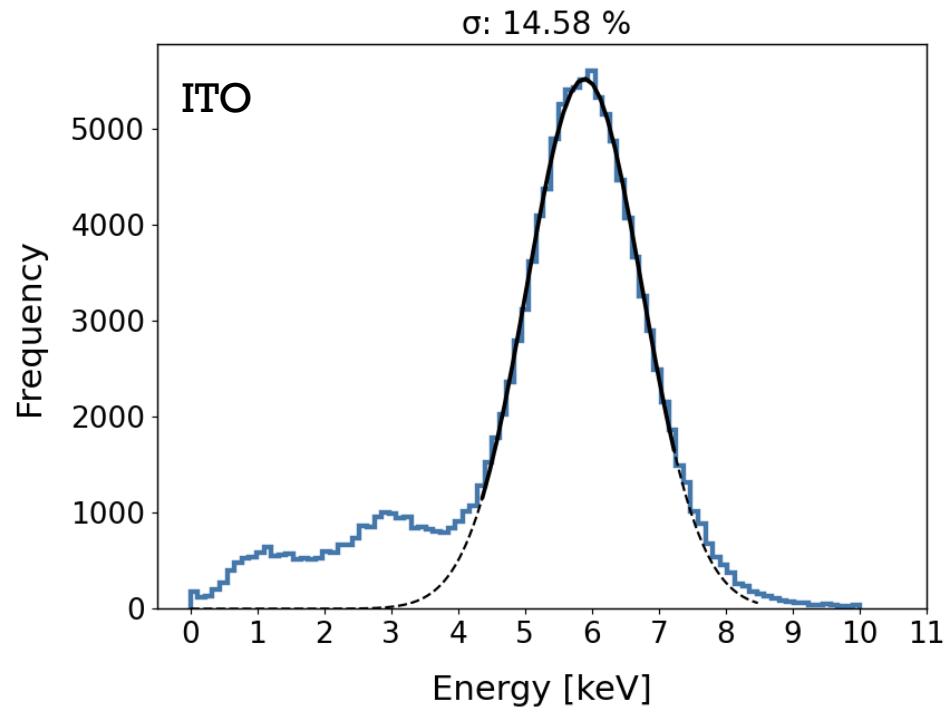
Calibration with ^{55}Fe – Ar / CF₄

- The chamber was tested with a fraction of argon at 50 Torr.
 - 20 % Ar / 80% CF₄
 - 30 % Ar / 70% CF₄
 - 40 % Ar / 60% CF₄
- Diffusion is greater.
- Tracks are in general longer.
- Stability is lower at high fractions of Ar.



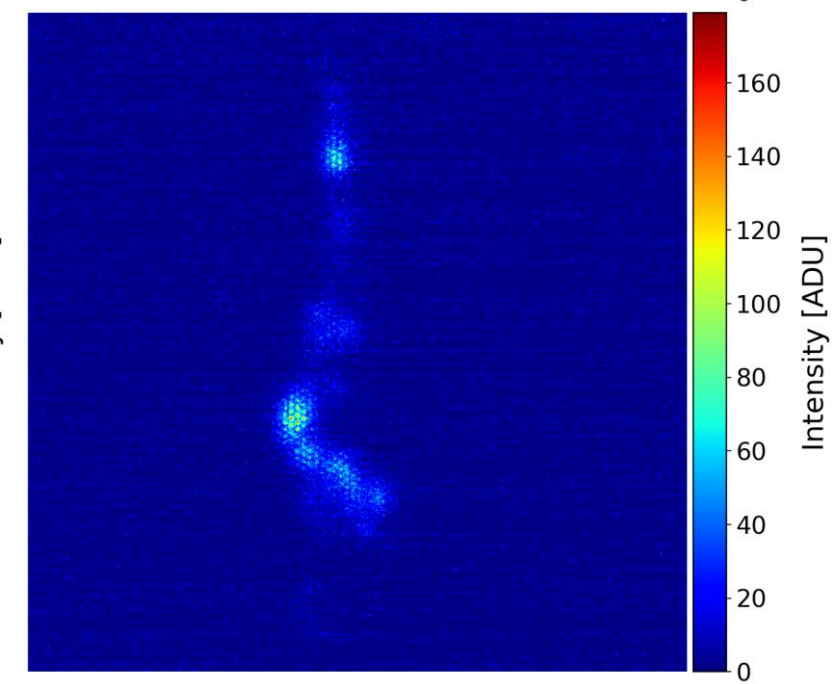
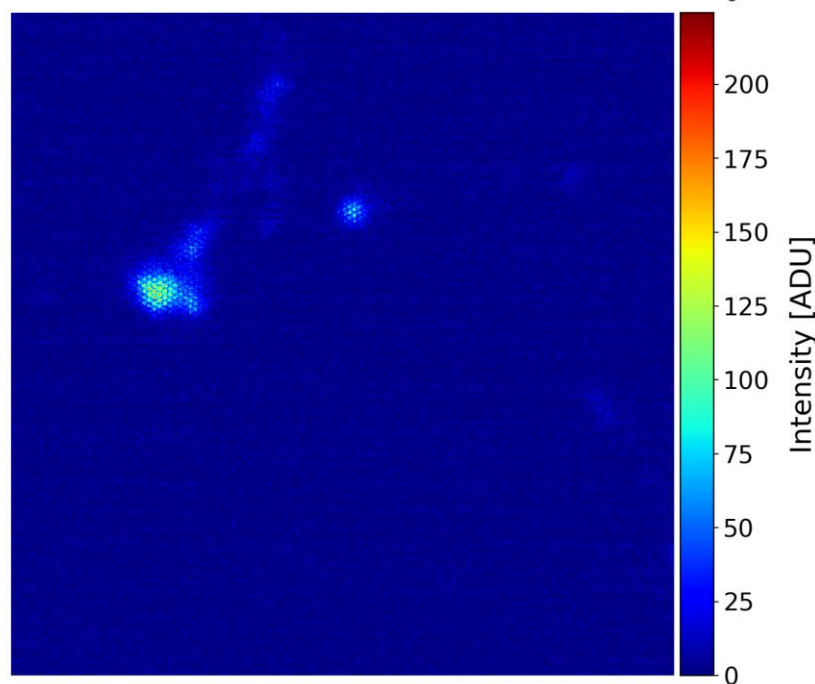
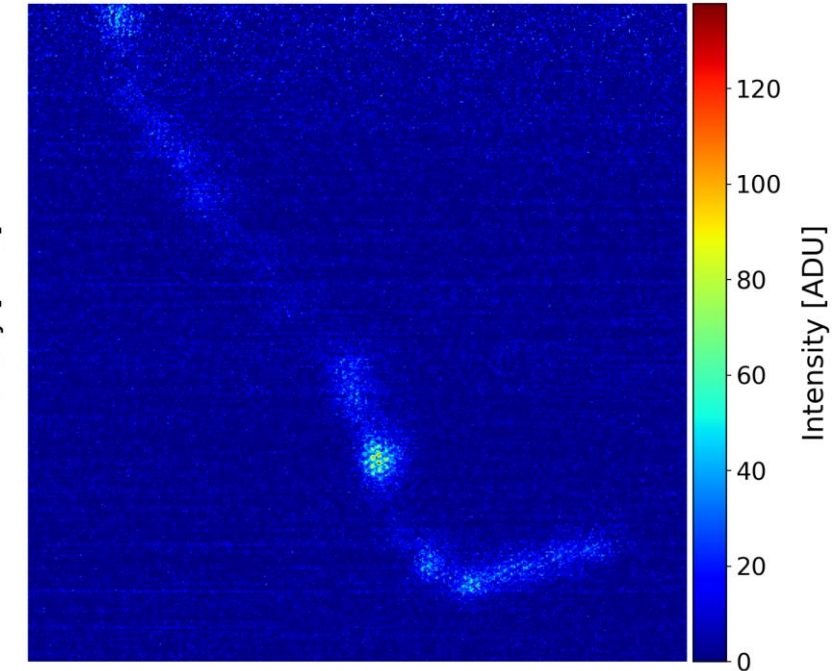
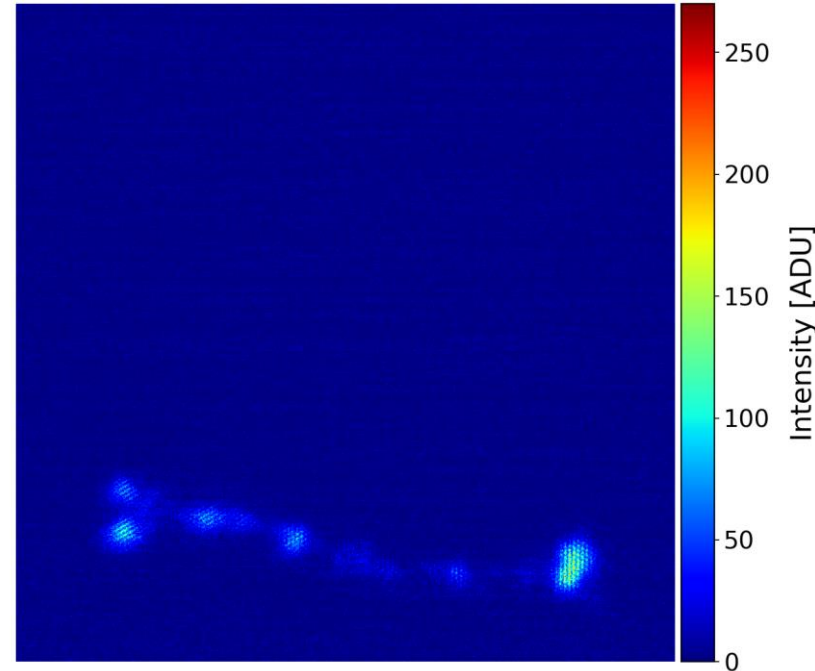
Energy resolution in Ar / CF₄

- Achievable energy resolution with fraction of Ar is comparable to pure CF₄.
- Second peak is resolved at 2.9 keV (escape peak).
 - X-ray from Ar
 - Independent photoelectron
- *See Elizabeth's talk on Thursday for more!*



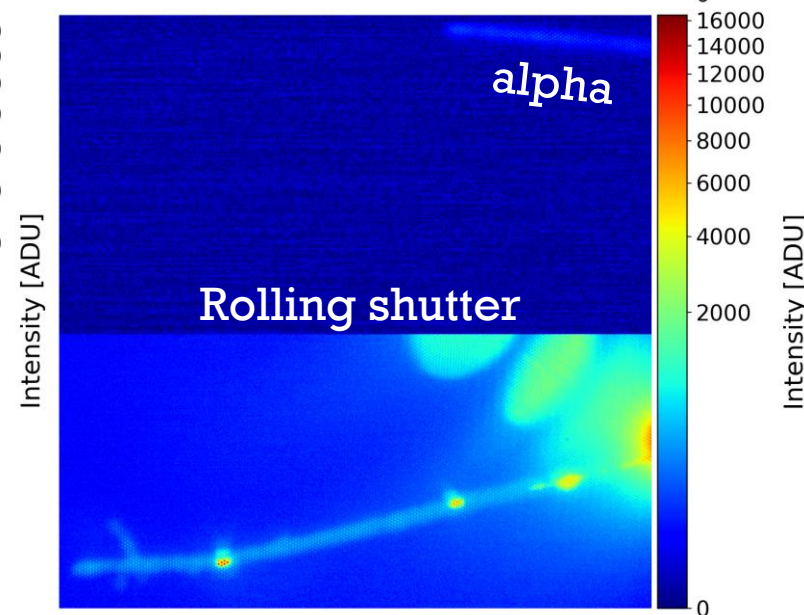
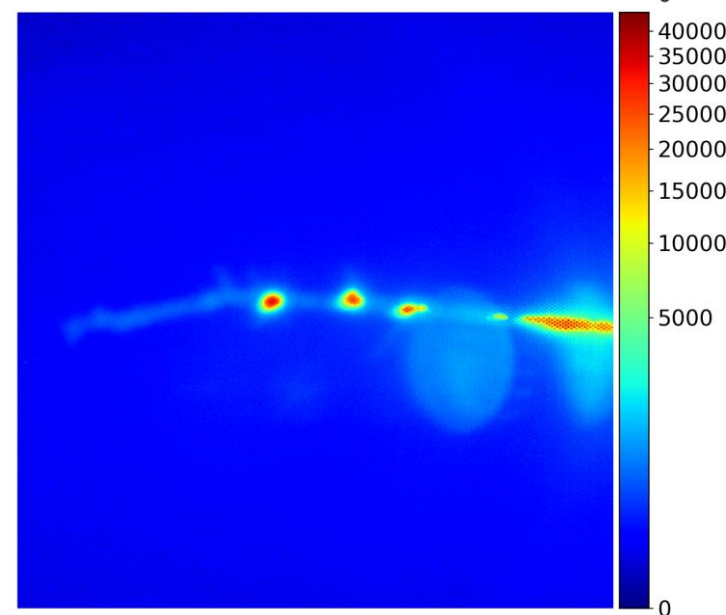
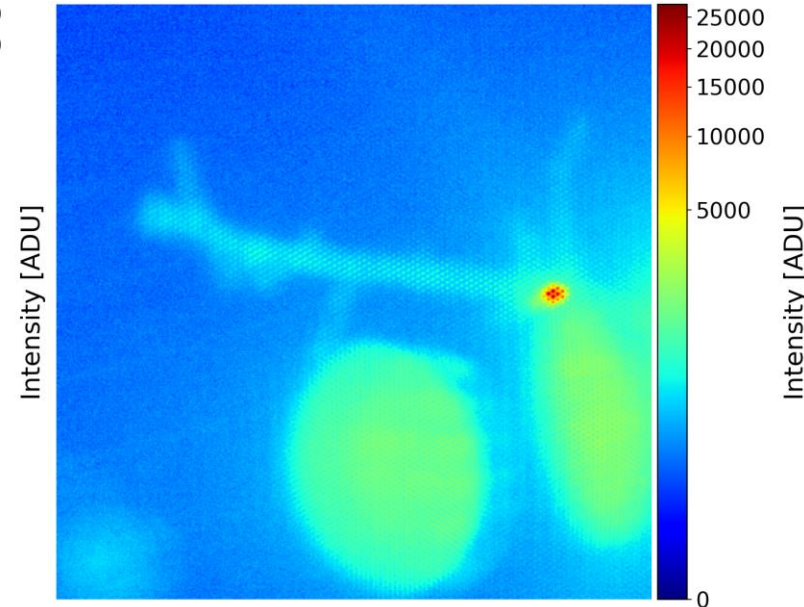
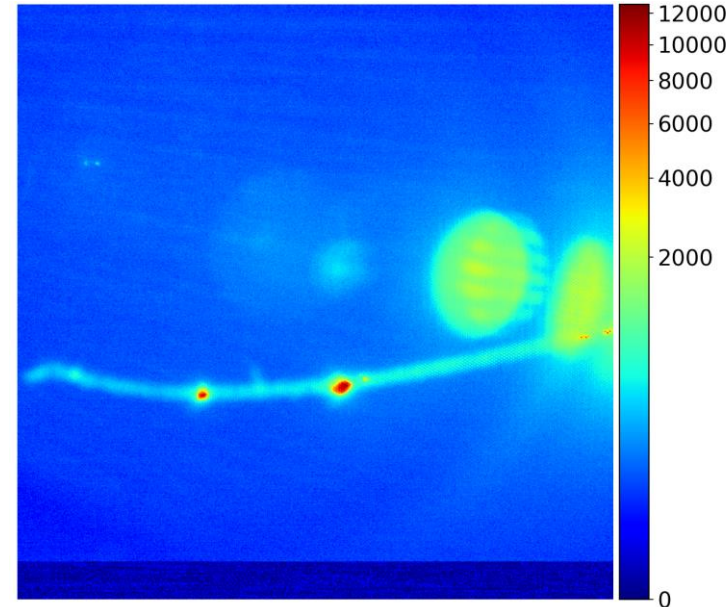
No source

- The detector sees high energy electrons with frequency ~ 1 Hz.
- Almost none of these tracks terminate in the active volume.
- Can see delta electrons emitted along the track.
- What is the source of these events? Electron shower?



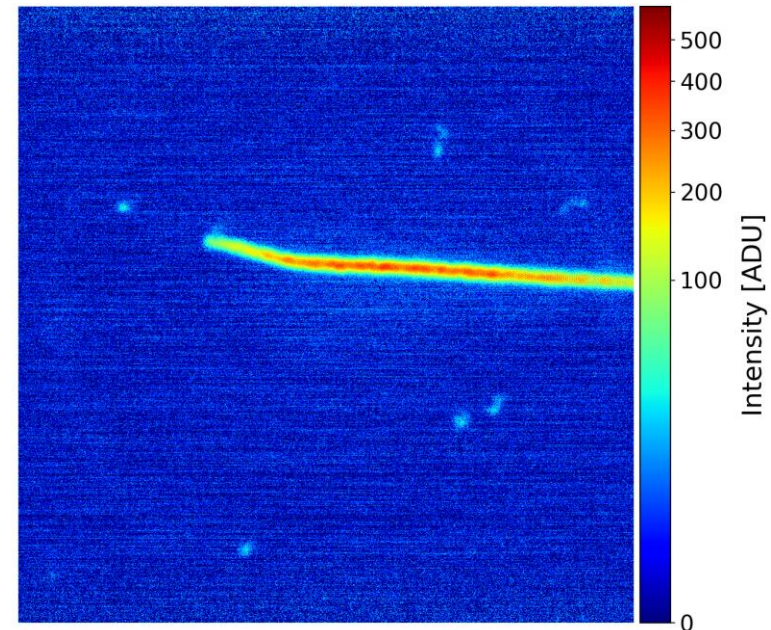
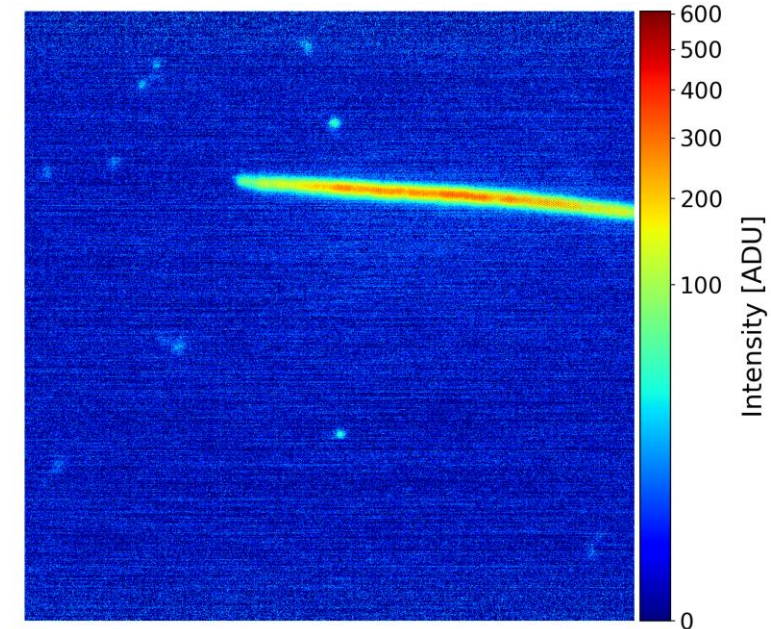
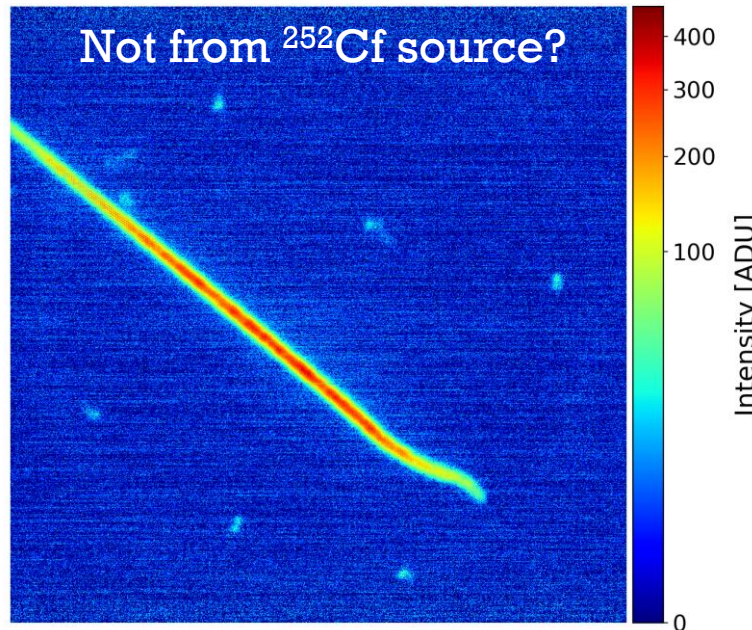
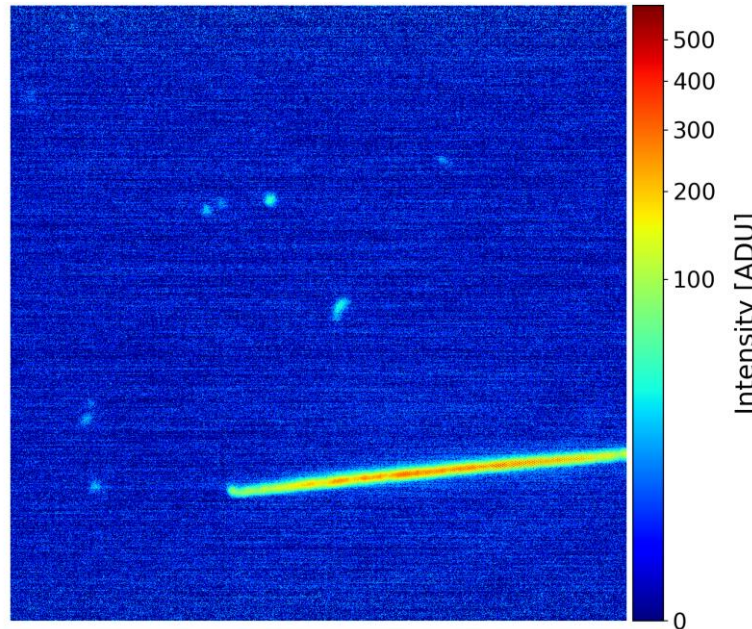
Fission fragments

- 37 Bq ^{252}Cf source was placed internally ~ 10 cm from active volume.
 - 6.2 MeV α
 - 80 MeV Nd
 - 105 MeV Pd
- Testing the dynamic range limits of the detector.
- At this distance the Nd/Pd have dE/dx comparable to nuclear recoil tracks produced by **DT (14.7 MeV)** neutron scattering.
- All fission fragment tracks produced sparks.



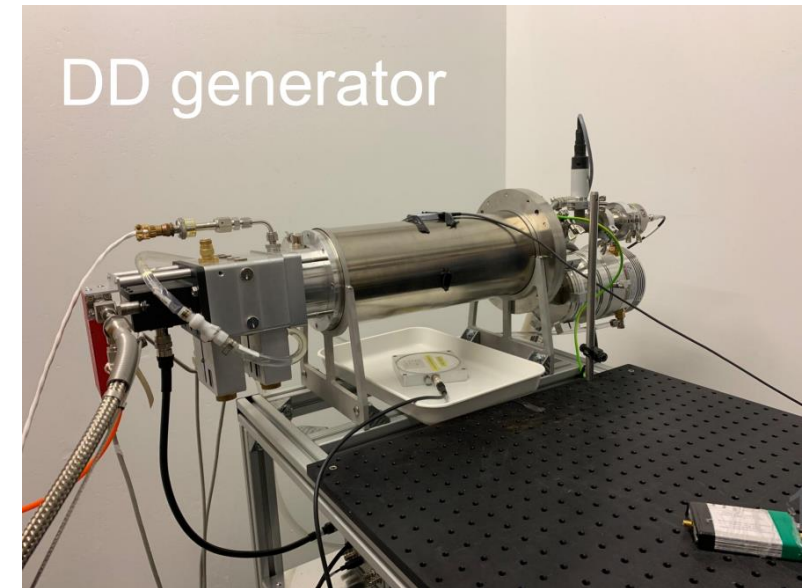
Alphas

- ^{252}Cf source was moved back to ~ 20 cm from active volume.
- At this distance Bragg peak for α terminates in the active volume.
- dE/dx comparable to nuclear recoil tracks produced by **DD (2.47 MeV)** neutron scattering.
- Can simultaneously observe α and 5 keV phe!



NILE facility

- NILE facility is at TS2, ISIS
- Test assembly of the lead & plastic shielding has been completed.
- DD generator is at NILE. We are awaiting its commissioning.

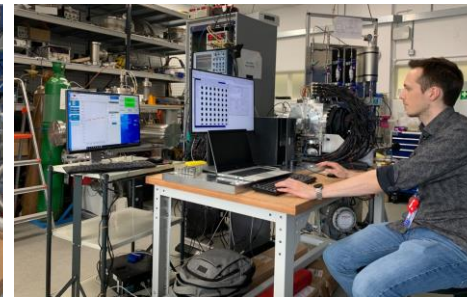
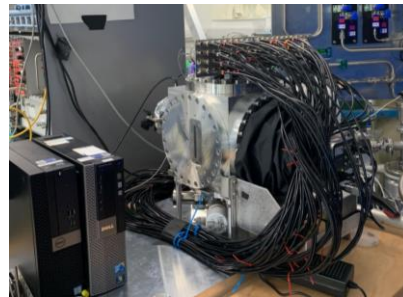


Summary

- The MIGDAL experiment aims to make a conclusive detection of the Migdal effect, followed by a systematic study: first in pure CF₄, then in other gases and mixtures.
- Design/sensitivity study completed ([2207.08284](https://arxiv.org/abs/2207.08284)), suggesting 5 σ discovery with 1 day.
- Optical-TPC has been built, now performing final tests and analysing calibration data: 5 keV threshold met.
- We are awaiting commissioning of the DD neutron generator.

Experiment paper: <https://arxiv.org/abs/2207.08284>

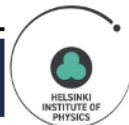
Please stay tuned on Thursday for Elizabeth's talk on 3D track reconstruction!



UNIVERSITY OF BIRMINGHAM



GDD
Gas Detectors Development Group



Imperial College
London

KING'S
College
LONDON



THE UNIVERSITY OF
NEW MEXICO



Rutherford Appleton Laboratory



Reserve slides

Papers

- [1] A. Migdal Ionizatsiya atomov pri yadernykh reaktsiyakh, ZhETF, 9, 1163-1165 (1939).
- [2] A. Migdal Ionizatsiya atomov pri α - i β -raspade, ZhETF, 11, 207-212 (1941).
- [3] M.S. Rapaport, F. Asaro and I. Pearlman K-shell electron shake-off accompanying alpha decay, PRC 11, 1740-1745 (1975).
- [4] M.S. Rapaport, F. Asaro and I. Pearlman L- and M-shell electron shake-off accompanying alpha decay, PRC 11, 1746-1754 (1975).
- [5] C. Couratin et al., First Measurement of Pure Electron Shakeoff in the β Decay of Trapped 6He^+ Ions, PRL 108, 243201 (2012).
- [6] X. Fabian et al., Electron Shakeoff following the β^+ decay of Trapped 19Ne^+ and 35Ar^+ trapped ions, PRA, 97, 023402 (2018).

ИОНИЗАЦИЯ АТОМОВ ПРИ ЯДЕРНЫХ РЕАКЦИЯХ

А. Мигдал

В работе вычисляется заряд новых отдачи при дезинтеграции, сопровождающихся передачей большой энергии.

При ядерных столкновениях или дезинтеграциях, сопровождающихся передачей большой энергии, должна происходить ионизация атомов отдачи. При малых скоростях ядра отдачи последнее успевает увлечь электроны, и ионизация не происходит; наоборот, при очень больших скоростях ядро вылетает из оболочки, не увлекая ее за собой. При не слишком больших энергиях отдачи ионизация происходит только в наружных, слабо связанных оболочках.

При столкновениях атомов с нейтронами такой механизм является единственным, приводящим к заметной ионизации (нетрудно убедиться, что ионизация, обусловленная магнитным и специфическим ядерным взаимодействием нейтрона с электроном, крайне мала — соответствующее сечение в первом случае порядка 10^{-25} см², во втором — порядка 10^{-30} см²).

Вероятность такой ионизации может быть очень просто рассчитана. Так как интересен случай больших энергий отдачи и, следовательно, больших скоростей падающей частицы, то время соударения с ядром много меньше электронных периодов. Следовательно, изменение скорости ядра происходит резко неадиабатически, так что Ψ — функция электронов — не может измениться за время столкновения.

Нетрудно, кроме того, видеть, что расстояние, на которое смещается ядро за время столкновения, имеет порядок $\frac{M_1}{M_2} R$, где M_1 — масса падающей частицы, M_2 — масса ядра, R — прицельное расстояние. Так как при заметной передаче энергии R много меньше размеров электронных оболочек, то ядро можно считать не сместившимся за время удара.

Для получения вероятности возбуждения или ионизации нужно исходную Ψ -функцию атома разложить по собственным функциям движущегося ядра. Можно поступить несколько иначе, и именно перейти к системе координат, в которой ядро покоится; тогда собственными функциями ядра будут обычные функции покоящегося ядра. Начальная функция Ψ_0 при этом преобразуется в выражение:

$$e^{i\mathbf{v}\cdot\mathbf{r}_i}\Psi_0(\mathbf{r}_1, \mathbf{r}_2, \dots, \mathbf{r}_f).$$

Действительно, множитель $e^{i\mathbf{v}\cdot\mathbf{r}_i}$ представляет собой Ψ -функцию центра инерции оболочки, который в старой системе координат покоился, а в новой движется со скоростью \mathbf{v} , равной по величине и противоположной по направлению скорости ядра.

Пусть конечное состояние атома в рассматриваемой системе координат дается функцией $\Psi_1(\mathbf{r}_1, \mathbf{r}_2, \dots, \mathbf{r}_f)$. Так как ядро за время удара не сместилось, то координаты электронов в Ψ_1 отсчитаны от той же точки, что и в Ψ_0 . Вероятность перехода в конечное состояние дается выражением:

$$W = \left| \int \bar{\Psi}_1 e^{i\mathbf{v}\cdot\mathbf{r}_i} \Psi_0 d\mathbf{r}_1 \dots d\mathbf{r}_f \right|^2, \quad (1)$$

Signal / background

Component	Topology	D-D neutrons		D-T neutrons	
		>0.5	5–15 keV	>0.5	5–15 keV
Recoil-induced δ -rays	Delta electron from NR track origin	≈ 0	0	541,000	0
Particle-Induced X-ray Emission (PIXE)					
X-ray emission	Photoelectron near NR track origin	1.8	0	365	0
Auger electrons	Auger electron from NR track origin	19.6	0	42,000	0
Bremsstrahlung processes [†]					
Quasi-Free Electron Br. (QFEB)	Photoelectron near NR track origin	112	≈ 0	288	≈ 0
Secondary Electron Br. (SEB)	Photoelectron near NR track origin	115	≈ 0	279	≈ 0
Atomic Br. (AB)	Photoelectron near NR track origin	70	≈ 0	171	≈ 0
Nuclear Br. (NB)	Photoelectron near NR track origin	≈ 0	≈ 0	0.013	≈ 0
Photon interactions					
Neutron inelastic γ -rays (gas)	Compton electron near NR track origin	1.6	0.47	0.86	0.25
Random track coincidences	Photo-/Compton electron near NR track	≈ 0	≈ 0	≈ 0	≈ 0
Gas radioactivity					
Trace contaminants	Electron from decay near NR track origin	0.2	0.01	0.03	≈ 0
Neutron activation	Electron from decay near NR track origin	0	0	≈ 0	≈ 0
Secondary nuclear recoil fork	NR track fork near track origin	–	≈ 1	–	≈ 1
Total background	Sum of the above components		1.5		1.3
Migdal signal	Migdal electron from NR track origin		32.6		84.2

[†] These processes were (conservatively) evaluated at the endpoint of the nuclear recoil spectra.

ER and NR tracks in 50 Torr CF₄

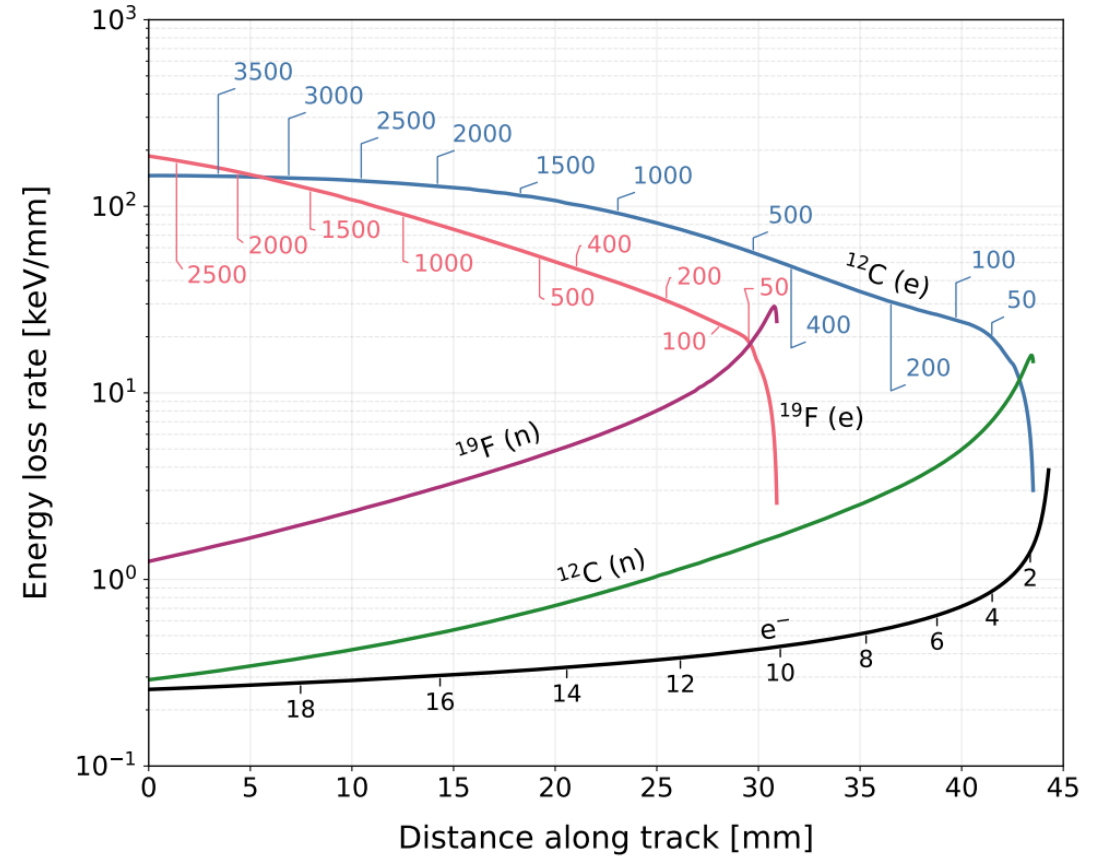
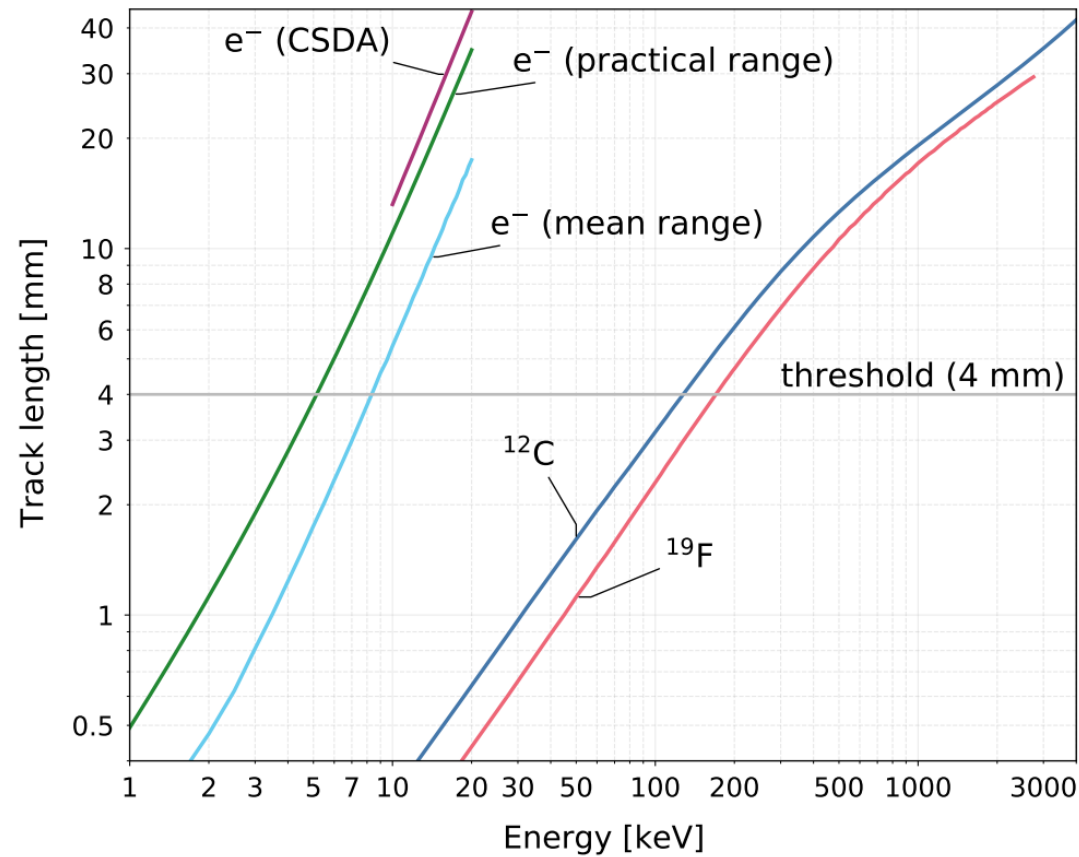


Figure 2: Left – Track length in CF₄ at 50 Torr for electrons (mean projected range calculated with Degrad [48], CSDA range with ESTAR [51], and the practical range formula from Ref. [52]), and mean projected range for carbon and fluorine ions from SRIM [49]). Right – Electronic and nuclear energy loss rates (CSDA) along carbon and fluorine ion tracks in CF₄ at 50 Torr, calculated with SRIM and electronic energy loss for 20 keV electrons obtained with ESTAR; called out values are interim particle energies (in keV) remaining at that point in the track.

Electron transport in 50 Torr CF₄

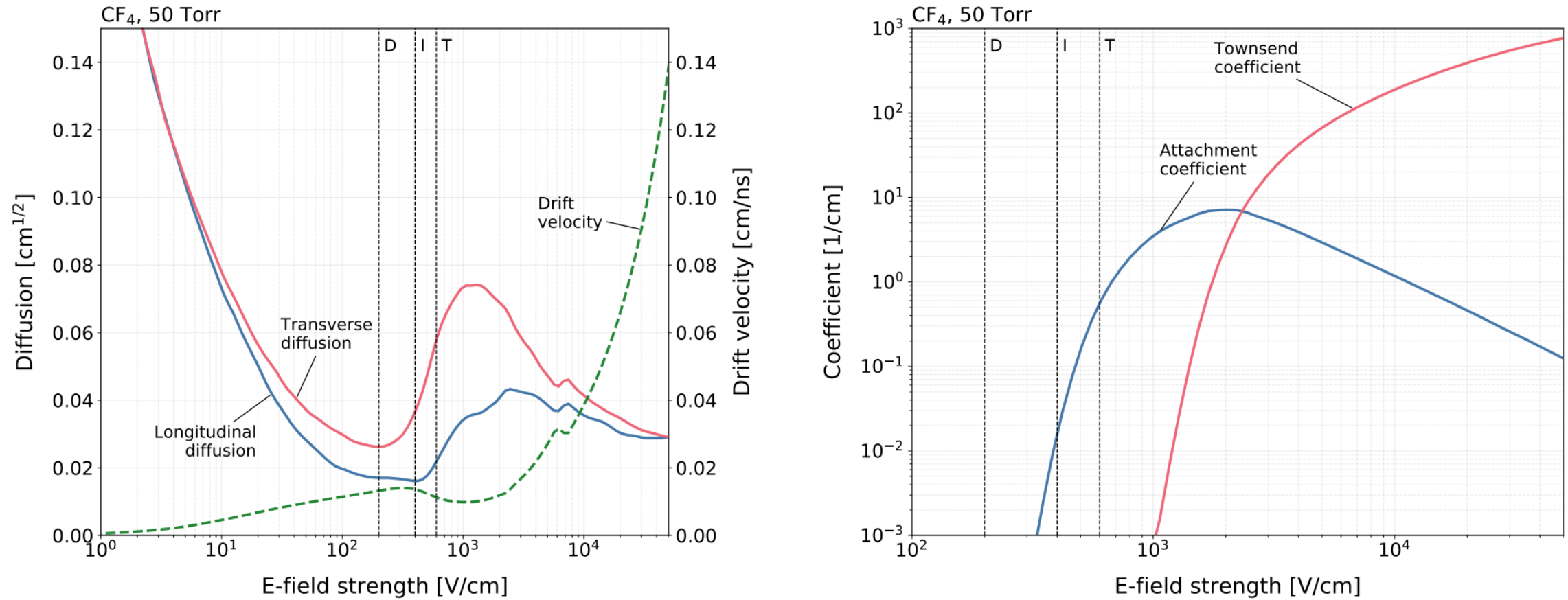


Figure 17: Electron transport properties of CF₄ at 50 Torr. Left – Drift velocity and diffusion. Right – Attachment and Townsend coefficients. Nominal fields in the drift (D), transfer (T) and induction (I) regions are indicated.

Migdal differential rates

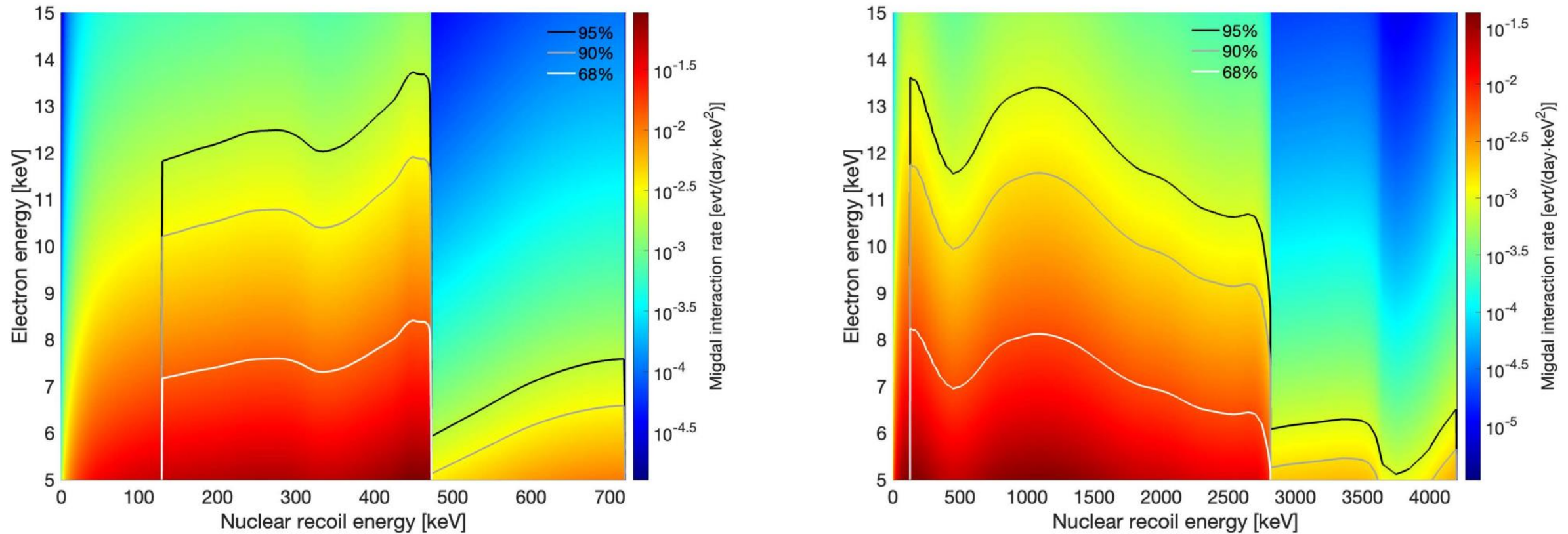


Figure 3: Double-differential Migdal rates for tracks contained in the OTPC from D-D (left) and D-T (right) generators. The contours are based on the NR thresholds of 130 keV and 170 keV for C and F, respectively. The area bound by the contours encompasses 68%, 90% and 95% of the signal.

Secondary nuclear recoils

Secondary recoils per million primary ions (TRIM) created within 1 mm from the vertex in 50 Torr CF_4 , when the “visible” energy of the secondary is 5–15 keVee.

Primary ion	Secondary ion	
Fluorine	Fluorine	Carbon
	500 keV	22,310 4,800
	400	26,840 5,930
	300	36,640 7,640
	200	56,130 1,263
	170	67,040 1,418
Carbon	Fluorine	Carbon
	500 keV	6,250 1,210
	400	7,950 1,610
	300	11,380 2,310
	200	17,310 3,700
	130	26,120 5,770

**~70,000
per million
(worst case)**

How many of these look like 5-10 keV electrons? Simulate several thousand more tracks using full chain, analyse image and recover track lengths (R_3) Can cut down to ~1 per 70,000 secondaries, retaining 87% electron detection efficiency (i.e. ~1 per million primary recoils).

